Electronic structure and phase stability of three series of B2 Ti-transition-metal compounds

1995 J. Phys.: Condens. Matter 7 6001

(http://iopscience.iop.org/0953-8984/7/30/006)

J. Phys.: Condens. Matter 7 (1995) 6001–6017. Printed in the UK

Electronic structure and phase stability of three series of B2 Ti–transition-metal compounds

J M Zhang† and G Y Guo‡

† Faculty of Mathematical Studies, University of Southampton, Southampton SO9 5NH, UK

‡ EPSRC Daresbury Laboratory, Daresbury, Warrington WA4 4AD, UK

Received 22 August 1994, in final form 1 March 1995

Abstract. Self-consistent electronic structure calculations have been performed for the 12 B2 TiM compounds (M = Fe, Co, Ni, Cu; Ru, Rh, Pd, Ag; Os, Ir, Pt, Au) using the linear muffin-tin orbital (LMTO) method. The calculated lattice constants and bulk moduli are in good agreement with measurements. An analysis of the possible correlations between the instability of the B2 structure and the electronic structures of the 12 TiM compounds has been carried out. The sequence of the B2 phase instabilities and the cubic → orthorhombic (or monoclinic) → orthorhombic (or monoclinic) → tetragonal tendency in the three TiM series have been discussed in terms of a band filling effect. The possible driving mechanisms of the structural phase transitions in the TiM series have been analysed based on the results of generalized susceptibility $X_0(q)$ calculations.

1. Introduction

A number of Ti-based binary compounds crystallize in the cubic CsCl (or B2) structure at high temperatures. However, they undergo a low temperature structural transformation from the cubic to an orthorhombic, or a monoclinic, or a hexagonal structure. The TiM compounds (where M stands for one of the transition elements in the three series—first: Fe, Co, Ni, Cu; second: Ru, Rh, Pd, Ag; third: Os, Ir, Pt, Au) can be considered as a celebrated representative of the family. It is interesting that their crystal structures tend to occur in nearly the same sequence when viewed as a function of the average number of valence electrons per atom, $\tilde{N}$ (see table 1). In table 1 valence electrons are calculated according to the periodic table. Therefore the average band filling varies from $\tilde{N} = 6$ to 7.5. Moreover some of the TiM compounds show an interesting pattern of structural modifications. Among the well studied ones are the cubic → tetragonal → orthorhombic sequence for TiRh (Chen and Franzen 1989) and cubic → trigonal → monoclinic for TiNi (Shapiro *et al* 1984, Shabalovskaya 1991). However, for TiCu with equal- or near-equal-atomic compositions, tetragonal structure has been found to be the only stable structure under various conditions (Karlsson 1951, Shabalovskaya and Narmonev 1988, Lutskaya and Alisova 1992).

TiNi is well known for its unique industrial application of the shape memory effect. The relationship between the phase instability and its electronic structure has long been the subject of intensive study. Shabalovskaya (1985) reviewed the work in the early 1980s and emphasized the role of electrons in the Ti de_g symmetry states in controlling the phase instabilities. The phase transformation in TiNi involves a series of intermediate phases and is followed by resistivity and specific heat anomalies as well as anomalies in phonon spectra and elastic constants along certain symmetry directions. Several attempts (Egorushkin and Kulkova 1982, Shapiro *et al* 1984, Zhao *et al* 1989) have been made to explain the anomalies

0953-8984/95/306001+17$19.50

Table 1. The observed low temperature crystal structures of the TiM compounds. $\bar{N}$ is the averaged number of valence electrons per atom, and M_s is the martensitic or martensitic-like transformation temperature. All the compounds (except TiCu and TiAg) show the B2 (CsCl) structure at high temperatures.

$\bar{N}$	1st series	2nd series	3rd series
6.0	TiFe B2 (CsCl)	TiRu B2 (CsCl)	TiOs B2 (CsCl)
6.5	TiCo[a] (hcp)	TiRh[b] NbRu orthorhombic structure	TiIr[c] A monoclinic structure with a value of β near 90°, or a NbRu orthorhombic structure
7.0	TiNi[d] B19 type M_s is about 45 °C	TiPd[d] B19 (AuCd) M_s is about 500 °C	TiPt[d] B19 (AuCd) M_s is about 1050 °C
7.5	TiCu[e] B11 (TiCu)	TiAg[e] B11 (TiCu)	TiAu[e] B11 (TiAu) or B19 (AuCd) The B2 to B11 or B19 transformation temperature is about 620 °C

[a] Not very clear. However, Shabalovskaya and Narmonev (1988) and Shabalovskaya (1989) reported that TiCo exhibits a B2 to hcp transformation at around 40 K.
[b] See, e.g., Chen and Franzen (1989).
[c] Not very clear. Some early reports indicated that α-TiIr had a monoclinic form with a value of β near 90° (see, e.g., Croeni *et al* (1962) and Eremenko and Shtepa (1970). Croeni *et al* (1962) reported that $\beta = 90°92'$ and Eremenko and Shtepa (1970) reported that $\beta = 90°52'$). However, Raman and Schubert (1964) reported that low temperature phase was NbRu orthorhombic.
[d] See, e.g., Shabalovskaya (1989, 1991).
[e] See, e.g., Massalski *et al* (1986).

based on the formation of a charge density wave (CDW) which is attributed to nesting in the Fermi surface. Eibler *et al* (1987) have carried out a comparative analysis of the chemical bonding properties of the three compounds, TiFe, TiCo and TiNi. They found that the density of states (DOS) of all three compounds shows two peaks, A and B, separated by a deep minimum. The band structures of these three compounds have been found to be similar and the decreased stability of the B2 structure was explained by an increased occupation of the antibonding states. Recently Shabalovskaya and co-workers (Shabalovskaya 1985, 1989, 1991, Shabalovskaya *et al* 1987, Shabalovskaya and Narmonev 1988) carried out systematic analysis on the possible connections between the instabilities of the B2 phases and the d band characteristics for a series of TiM compounds. The structural instability of B2 was then assumed to be connected with the degenerate Ti d states at the Fermi level.

Several electronic structure calculations have been carried out for the TiNi compound (Egorushkin and Kulkova 1982, Eibler *et al* 1987, Zhao *et al* 1989, Kulkova *et al* 1991, Bihlmayer *et al* 1992). Electronic structure calculations have also been performed for B2 TiFe (Papaconstantopoulous 1975, Papaconstantopoulous *et al* 1982, Eibler *et al* 1987), for B2 TiCo (Eibler *et al* 1987), for B2 TiRh (Folkerts and Haas 1989) and for B2 TiPd (Naumov *et al* 1991, Bihlmayer *et al* 1992), but not for B2 TiRu, B2 TiOs, B2 TiIr, B2 TiPt, B2 TiAu and unstable B2 TiCu and B2 TiAg. An overall comparative analysis of the B2 phase instabilities in all three series of TiM compounds based on the electronic structure calculations is still lacking. The primary objective of the present paper is to find

out the relationship between the instabilities of the B2 phases in the three series and the features of their electronic structures. We have calculated the electronic structures of all three series. Based on the results obtained, we want to understand why the three series show similar behaviours as $\tilde{N}$ goes from 6 to 7.5 (table 1). Our second purpose lies in the study of dynamic mechanisms of phase instabilities. Some of the TiM compounds in the series can exist in diversified modifications. As dynamic behaviours largely depend on the subtle features of electronic structures, it is hopeful that first-principles calculations may help to gain insight at the microscopic level.

The paper is organized as follows. First, in section 2 we describe aspects of our electronic structure calculations. In section 3.1 we compare the theoretical results of lattice constants and bulk moduli for the 12 B2 TiM compounds with experiments. In section 3.2 we show the calculated electronic band structures (BS), densities of states (DOS) and Fermi surfaces (FS) for the 12 B2 TiM compounds, discuss the major factors determining the basic features of BS, DOS and FS, and try to relate the cubic → orthorhombic (or monoclinic) → orthorhombic (or monoclinic) → tetragonal tendency in the three TiM series to their electronic structure characteristics. In section 3.3 the calculated generalized susceptibility in the [110] and [100] directions of the 12 B2 compounds are presented and discussed in conjunction with the study of the driving mechanisms and the relationship between certain phase modifications and the subtle features of the Fermi surfaces and the peculiarities in the electronic energy bands. In section 3.4 the results of the electronic structure calculations of the low temperature phases for some of the TiM compounds are reported. Finally, in section 4, we summarize our findings about the relationship between the phase instabilities in the three TiM series and their electronic structures, and the main factors in determining the basic features of the electronic structures.

2. Calculated aspects

Self-consistent band structure calculations of 12 ordered B2 TiM compounds have been performed using the standard linear muffin-tin orbital method with the atomic sphere approximation (LMTO-ASA) (Andersen 1975, Skriver 1984). Combined correction terms have been included in order to obtain more accurate results. These calculations are based on the density functional theory of Hohenberg, Kohn and Sham (Hohenberg and Kohn 1964, Kohn and Sham 1965) with the local density approximation. The von Barth–Hedin local density form for the exchange and correlation potential (von Barth and Hedin 1972) has been used throughout. The valence states (3d, 4s and 4p for first series; 4d, 5s and 5p for second series; and 5d, 6s and 6p for third series) have been iterated in the self-consistency cycles, whereas the frozen core approximation has been assumed for the remaining lower states. The cubic B2 structure contains two atoms per unit cell, i.e. one Ti and one M. The calculations have been performed with a mesh of 680 k-points in the irreducible wedge (1/48) of the simple cubic Brillouin zone (IBZ). The results are well converged with respect to the number of k-points. The variation of the total energy from iteration to iteration is less than 1×10^{-5} Ryd. Moreover, in the Fermi surface calculations a much finer grid of 5456 k-points in the IBZ has been used. The total and partial DOS have been determined by means of the tetrahedron method (see Lehman and Taut 1972). In the generalized susceptibility calculations a similar tetrahedron technique proposed by Rath and Freeman (1975) has been used.

Table 2. Theoretical and experimental lattice constants for the B2 TiM compounds. $\tilde{N}$ is the average number of valence electrons per atom.

$\tilde{N}$	*Compounds*	*Theoretical lattice constants (Å)*	*Experimental lattice constants (Å)*
6.0	TiFe	2.987	2.97 (Nevitt 1963) 2.976 (Brandes and Brook 1992) 3.0 (Shabalovskaya 1991)
	TiRu	3.137	3.06 (Brandes and Brook 1992) 3.07 (Nevitt 1963)
	TiOs	3.151	3.07 (Brandes and Brook 1992)
6.5	TiCo	2.999	2.99 (Brandes and Brook 1992) 3.012 (Shabalovskaya 1991)
	TiRh	3.150	3.126 (Yi *et al* 1988)
	TiIr	3.164	3.125 for $Ti_{65}Ir_{35}$ (Raman and Schubert 1964)
7.0	TiNi	3.023	3.01 (Smithells 1962) 3.015 (Brandes and Brook 1992) 3.04 (Shabalovskaya 1991)
	TiPd	3.191	3.18 (Donkersloot and Van Vucht 1970)
	TiPt	3.205	3.192 (Donkersloot and Van Vucht 1970)
7.5	TiCu	3.074	
	TiAg	3.259	
	TiAu	3.267	3.252 (Donkersloot and Van Vucht 1970)

3. Results and discussion

3.1. Lattice constants and bulk moduli

In table 2, calculated lattice constants are compared with measurements. As we can see, they are in good agreement with experiments. In figure 1, the theoretical and experimental bulk moduli are plotted against $\tilde{N}$ and they are in reasonably good agreement. As $\tilde{N}$ runs from 5 to 7.5, the theoretical results show a parabolic behaviour. For many of the transition-metal-based alloys with $\tilde{N}$ exceeding the value of $\tilde{N} = 6$, their B2 phases would become unstable. This would make measurements of bulk moduli difficult. This perhaps explains why experimental data for $\tilde{N}$ greater than 6 are rare. Nevertheless, some researchers (see, for instance, Colling and Gegel 1975, Shabalovskaya 1991) argued that when $\tilde{N}$ goes beyond 6 the bulk modulus curve should experience a parabolic fall, similar to the theoretical curves shown in figure 1.

3.2. Band structure, density of states and Fermi surface

Generally speaking, the band structure (BS) and DOS of the 12 TiM compounds are similar to each other. Two main peaks A (the lower energy one) and B (the higher energy one) exist and are separated by a deep minimum. For the compounds with isoelectronic elements the BS and DOS are almost identical and therefore in most cases we show only one representative for each triplet. The representatives of the band structure (BS) are displayed in figure 2, the total and site-decomposed DOS in figure 3, and the Fermi surfaces (FS) in figure 4. The A peak is dominated by the M d DOS with an admixture of a relatively small

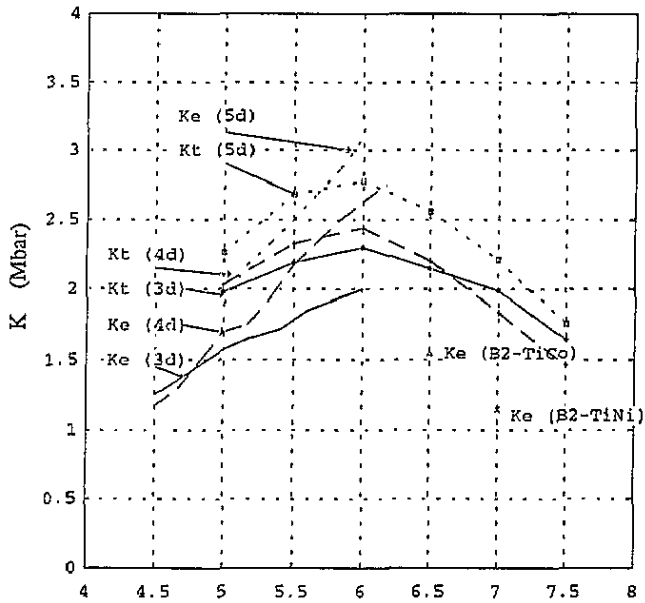

Figure 1. Bulk modulus K vs. the averaged valence electrons per atom, $\tilde{N}$. Subscript t denotes theoretical curves, and subscript e denotes experimental ones. Curves K_e (3d, 4d and 5d) are from Katahara *et al* (1979a, b) and Fisher and Dever 1970); K_e (B2 TiCo) is from Yasuda *et al* (1991); and K_e (B2 TiNi) is calculated from the data given by Brill *et al* (1991).

part of the Ti d DOS which decreases as the empty bands of the M components become progressively filled. The B peak is mainly formed by the Ti d states with an admixture of a small part of the M d states which decrease as $\tilde{N}$ changes from 6 to 7.5. There are clear signs of the band filling effect. The stability of the B2 structure of TiFe, TiRu and TiOs could be explained by the fact that their Fermi levels are positioned in the valley separating the 'bonding states' (A peak) and 'antibonding ones' (B peak). The decreased stability with the increase of $\tilde{N}$ could be accordingly attributed to the gradual occupation of the antibonding states. Moreover, our results for B2 TiCu, B2 TiAg and B2 TiAu, as shown in figure 3 for B2 TiCu as a representative, indicate that the singularity in the B peak is responsible for the phase instability observed. For B2 TiCu and B2 TiAg the Fermi levels lie on the sharp singular peak with $\mathrm{DOS}(E_f) = 73.89$ and $\mathrm{DOS}(E_f) = 68.47$ (states Ryd^{-1}/cell) respectively. However for B2 TiAu the Fermi level narrowly misses the sharp peak with $\mathrm{DOS}(E_f) = 56.99$ and the B2 structure is stable at high temperatures. Inspection of the partial DOS reveals that the singularity in the DOS of TiCu and TiAg comes from mainly the Ti de_g state. The instability of the electronic structure with its Fermi level lying in the middle of a degenerate singularity can be understood by an electronic band energy gain through the Jahn–Teller effect.

Figure 5 shows some important features of the band filling. As can be seen from figure 5, when $\tilde{N}$ runs from 6 to 7.5, the partial Ti charge stays constant and the additional electrons go exclusively into the M site. With M becoming more like a filled sphere with 10 d states gradually occupied, its d electrons become more and more localized and its electronic dispersion curves become less willing to hybridize with other bands. Consequently, the

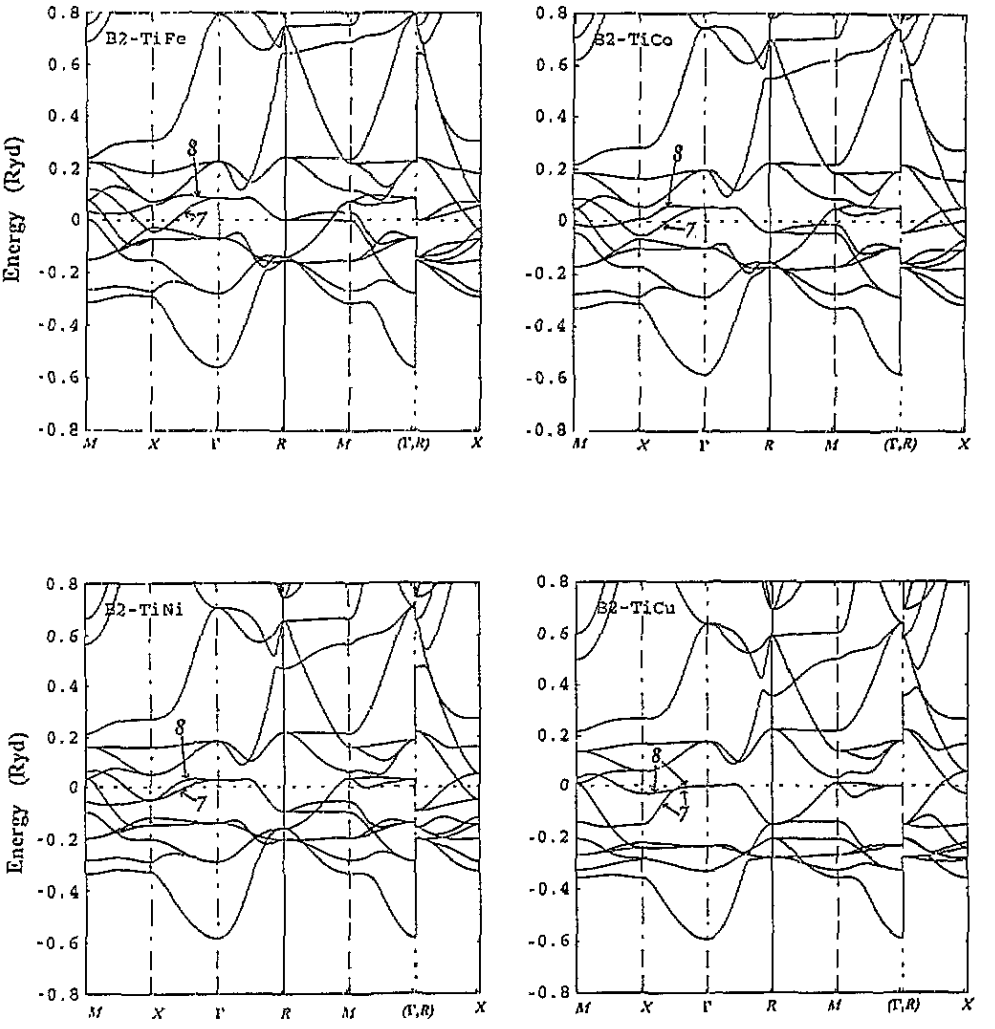

Figure 2. Electronic band structures for the selected B2 TiM compounds. The Fermi level, E_f, has been designated to be at $E = 0$.

bands become narrower. This is most clearly visible for the M d bands. The M d-state filling effect has reduced the widths of the M d bands to a half of the original size when $\tilde{N}$ goes from 6 to 7.5. However it has less influence on the Ti d bands as the widths of the Ti d bands have only been reduced by about one-sixth. The M d-state filling effect is perhaps the major factor in shaping the overall appearance of the BS and DOS as it plays an important role in determining how strong the hybridization of the electronic states from different atoms is and how large the energy difference of the electronic states split by the ligand-field effect is. This is due to the fact that, in the case of the TiM compounds, the Ti energy levels are well above that of the M's. If the M d states were highly localized, as in the cases of TiCu and TiAg, Ti d electrons would drop down to the unfilled part of the M d states, the electron distribution around the Ti sphere and M sphere would become severely unbalanced, and the electrostatic field would act to resist the charge transfer. As a trade-off

of these two competing forces the unoccupied M d bands will be driven upwards and the M d electrons from different bands would be strongly hybridized with the Ti d electrons. For $\tilde{N} = 6$ and $\tilde{N} = 6.5$, the upward movements of the M d $E(k)$ curves are most visible and the d–d hybridizations are strongest. As the M d states become progressively filled, the effect gradually fades away and down to a minimum at $\tilde{N} = 7.5$.

Inspection of the BS and DOS (figures 2 and 3) can be helpful for determining the components of the electronic orbital which control the phase stabilities. In the antibonding peak B there is a sub-antibonding peak (SAPK) which can be identified as responsible for the B2 phase instabilities. This sub-peak immediately rises from the valley. For all the compounds with $\tilde{N} = 6.5$ to 7.5, E_f is located in the SAPK. As discussed above, the B peak is formed by the Ti d states with an admixture of a small part of M d states. As this small part of the M d electrons is concentrated in the SAPK, these M d states play an important role in determining the phase instabilities in most TiM compounds. With the M d electrons becoming more localized the M d state contribution in the SAPK gradually fades away. As a result, for TiCu and TiAg, the SAPK becomes dominated by the Ti d e_g electrons. This phenomenon is less clearly visible for the partial Ti d DOS and also it happens in the opposite direction. The filling behaviour of the partial d bands displayed in figure 5 is surprising. While E_f moves up towards the antibonding peak, the Ti d NOE(E_f), in contrast, gradually decreases (where NOE(E_f) is the number of electrons occupying the states up to E_f). Shabalovskaya (1985, 1991), Shabalovskaya *et al* (1987) and Shabalovskaya and Narmonev (1988) argued that, for B2 TiM, E_f is dominated by the Ti d states which control the phase stability. Our results however suggest a more complicated picture. We find that for the $\tilde{N} = 6.5$ group and even the $\tilde{N} = 7$ group, the Ti d states and M d states have a nearly equal contribution to the total DOS(E_f). Only for the compounds of B2 TiCu, B2 TiAg and B2 TiAu can one say that DOS(E_f) is dominated by the d electrons from the Ti site. For $\tilde{N} = 6.5$ and $\tilde{N} = 7$ the M d states are the main constituent to form the SAPK. Only for $\tilde{N} = 7.5$ with the M d electrons largely localized can one say that the SAPK is dominated by the electrons from Ti d e_g states.

The B2 → orthorhombic (or monoclinic) → orthorhombic (or monoclinic) → tetragonal sequence shown in table 1 may be explained in terms of the band Jahn–Teller effect. For the e_g state the cubic to tetragonal phase transformation has little effect on orthorhombic instability. However, for t_{2g} triplet states the transformation to a tetragonal phase may enhance the instability towards an orthorhombic distortion. For $\tilde{N} = 6.5$ the M d NOE(E_f) is less than 8 and for $\tilde{N} = 7$ less than 9, and the Ti d NOE(E_f) is around 2 for both $\tilde{N} = 6.5$ and 7. In these cases the Ti t_{2g} and M t_{2g} states make a large contribution to the formation of the SAPK and consequently an orthorhombic phase would be more stable than a tetragonal one. For B2 TiCu and B2 TiAg, the SAPK is dominated by the Ti d e_g state and the energy gain would be mainly due to the splitting of the Ti d e_g state which has little impact on the orthorhombic instability. In this case a tetragonal phase may exist stably at low temperatures. For B2 TiAu with 9.2 Au d states occupied, there is a possibility for an orthorhombic phase to have lower energy than a tetragonal one. Such transformation to an orthorhombic phase (B19) has been found in compositions less than 50 at.% Au (Massalski *et al* 1986, Shabalovskaya 1991).

Finally, we discuss the electronic structures obtained by other researchers. Papaconstantopoulos (1975) and Papaconstantopoulos *et al* (1982) and Eibler *et al* (1987) have utilized the augmented plane-wave (APW) method to calculate the electronic structures for B2 TiFe, B2 TiCo and B2 TiNi. Their results of the BS and DOS are in good agreement with ours. Kulkova *et al* (1991) and Naumov *et al* (1991) have published the total DOS for B2 TiNi and the Fermi surface for B2 TiPd and B2 TiPt using the LMTO-ASA method. Not

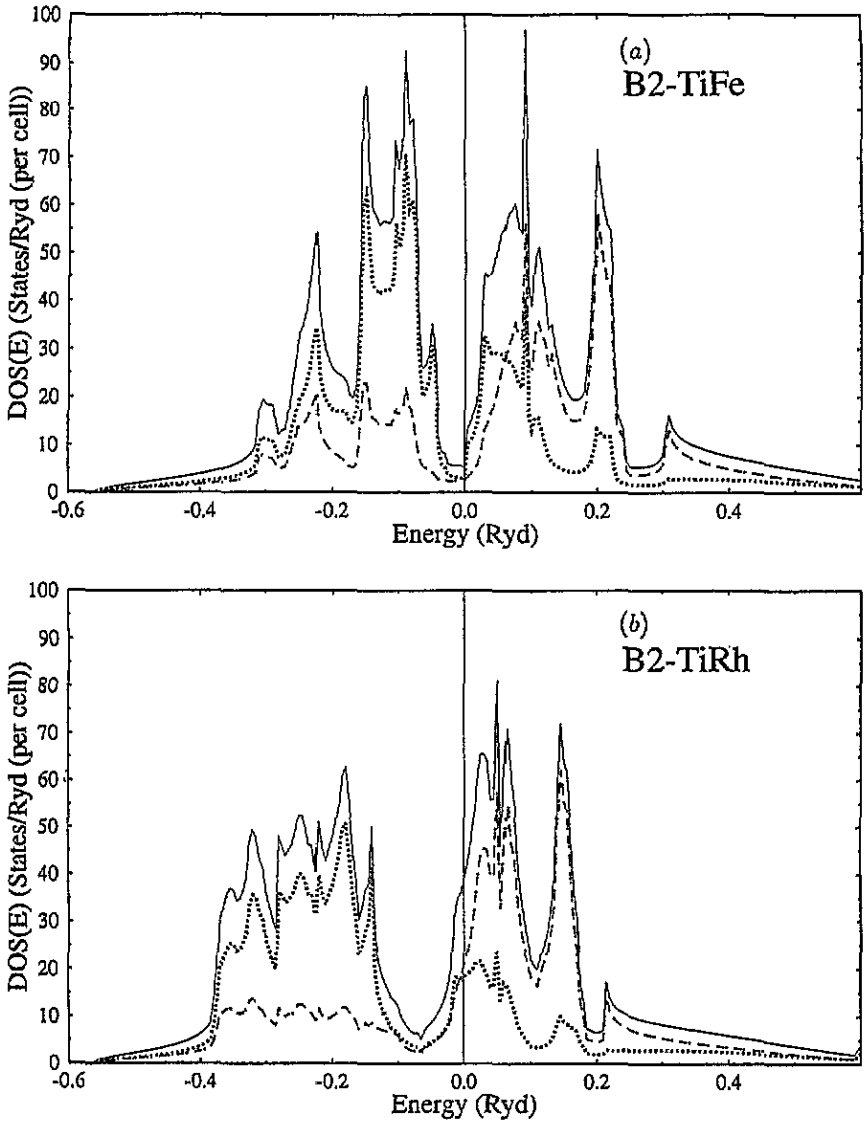

Figure 3. Density of states, DOS(E), for the selected B2 TiM compounds. The Fermi level, E_f, has been designated to be at $E = 0$. Full curve, total DOS; chain curve, Ti-site DOS; dotted curve, M-site DOS.

surprisingly, their results agree well with ours. More recently comes the work for B2 TiNi and B2 TiPd by Bihlmayer *et al* (1992) also using the linear APW (LAPW) method. Again, the results of Bihlmayer *et al* (1992) are very similar to ours. Finally, a good agreement is found between figure 4 and the Fermi surface contour plot for B TiNi by Zhao *et al* (1989) using the tight-binding method.

3.3. Susceptibility

There is a large category of structural phase transitions which are caused by the destabilizing electrons around the Fermi level. The generalized susceptibility $X_0(q)$ of wavevector q for

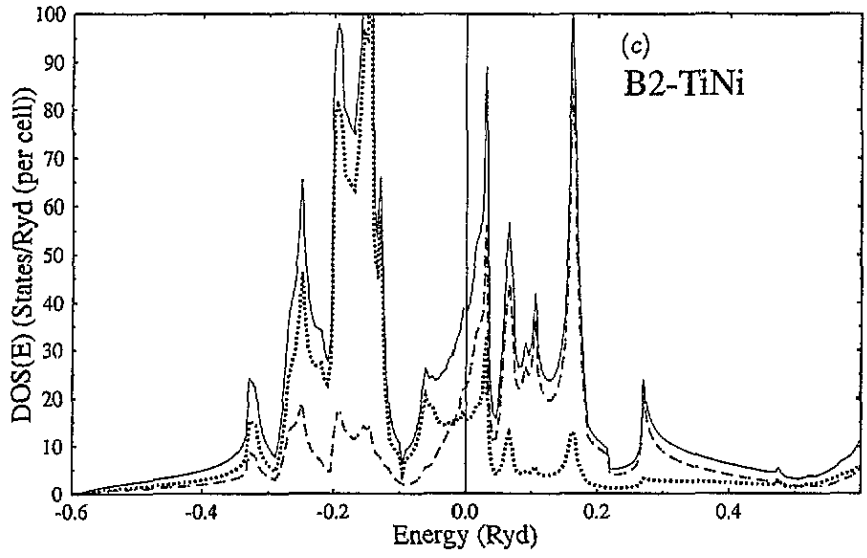

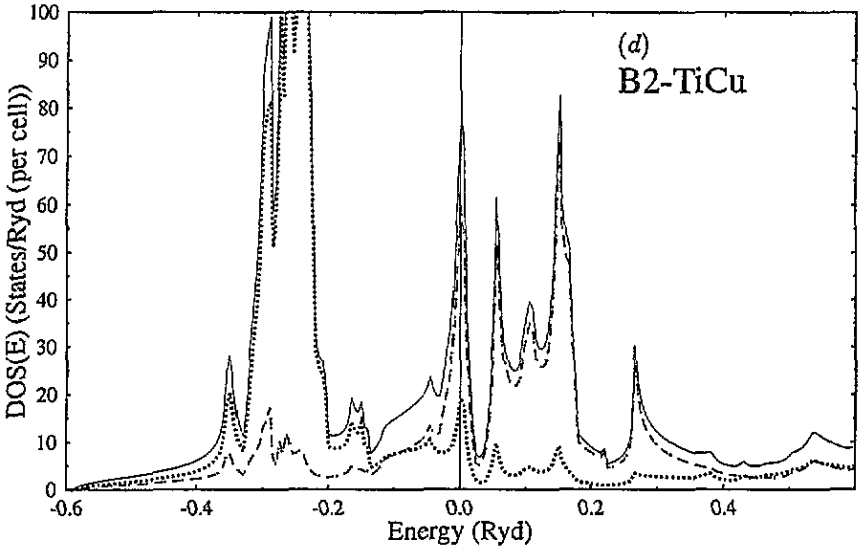

Figure 3. (Continued)

a non-interacting electronic system is given by the following equation:

$$X_0(q) = \frac{2\Omega}{(2\pi)^3} \int \mathrm{d}k \sum_{j,j'} \frac{f(E_j(k))[1 - f(E_{j'}(k+q+O))]}{E_{j'}(k+q+Q) - E_j(k)}.$$

It is well known that this quantity is useful for detecting such electronic anomalies (see, e.g. Nakanishi 1979, Shabalovskaya 1985, Naumov *et al* 1991). A sharp peak in $X_0(q)$ is often associated with lattice instabilities. For example for a given phonon q the electron–phonon coupling can be sufficiently enhanced to generate a charge density wave (CDW) and to cause an instability if $X_0(q)$ peaks at q. However there exist other types of lattice instabilities which could also be traced back to the singularities in $X_0(q)$. This can be seen

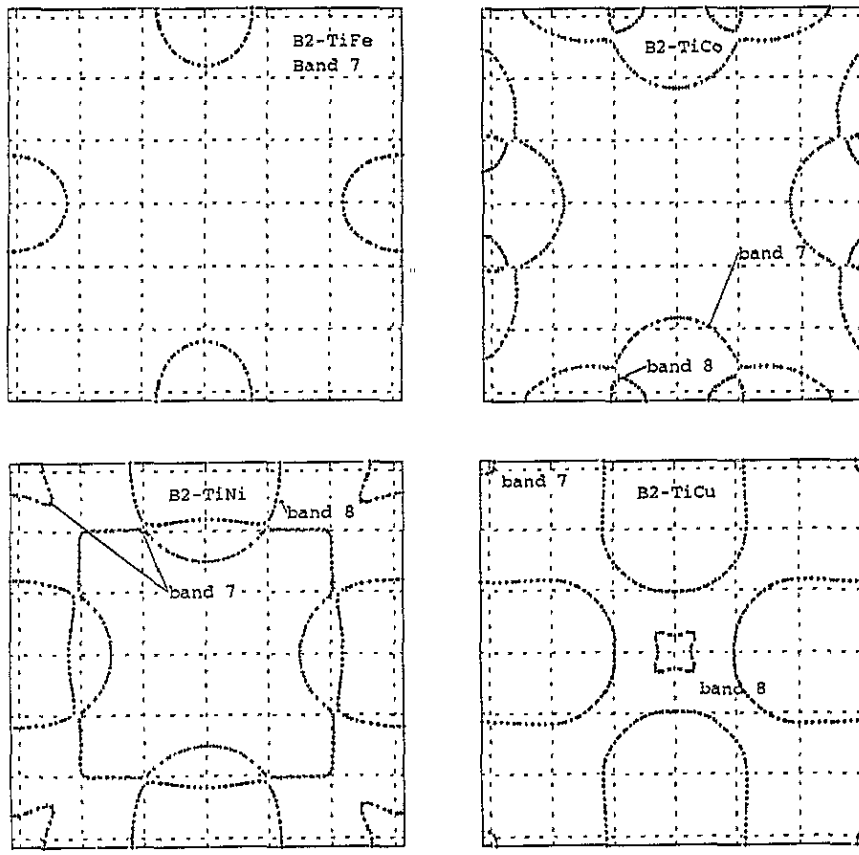

Figure 4. The Fermi surface in the [100] plane for bands 7 and 8 for the selected B2 TiM compounds.

in the cases of B2 TiCi and B2 TiAg. In figures 6 and 7 some representative results for q along [100] and [110] directions have been displayed. For the $\tilde{N} = 6$ group $X_0(q)$ shows small values and no peak can be detected. For the $\tilde{N} = 6.5$ group for q along [110], small peaks appear in the region from $Q_0 = (0.1, 0.1, 0)2\pi/a$ to $Q_0 = (0.15, 0.15, 0)2\pi/a$. For q along [100], B2 TiCo is the only member showing a small peak around $(0.15, 0, 0)2\pi/a$. They may not be related to the phase transformations observed in these compounds. For the $\tilde{N} = 6.5$ group, our results along [110] direction are nearly the same as that reported by Zhao *et al* (1989) for B2 TiNi and by Naumov *et al* (1991) for B2 TiPd and B2 TiPt. The observation of the peaks has been used to support a CDW driving mechanism for the phase transition from the cubic to an incommensurate phase (IC) prior to the martensitic transformations in these compounds (Zhao *et al* 1989, Naumov *et al* 1991).

The results for B2 TiCu and B2 TiAg in both the [100] and [110] directions show a tendency towards a high peak as q approaches zero. Unexpectedly, this feature in $X_0(q)$ cannot be detected from the Fermi surface plotting. Analysis of the partial contributions shows that these peaks stem from transitions between bands 7 and 8. However, the cross-section in figure 4 for B2 TiCu shows that band 7 only has small pockets around the M point and no sign of nesting exists. This also holds for B2 TiAg. The singularity in the $X_0(q)$ curves for TiCu and TiAg around $q = 0$ actually does not come from the Fermi surface nesting. Inspection of the BS and DOS for TiCu and TiAg shows that Cu (Ag)

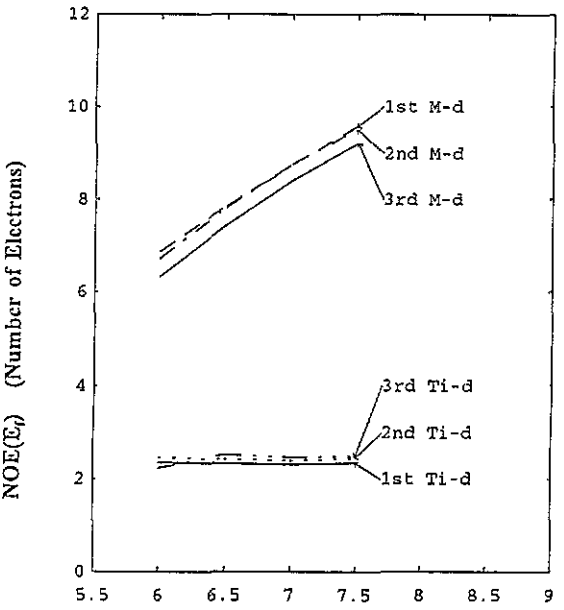

Figure 5. Partial d NOE(E_f) of M and Ti in B2 TiM for the three series of TiM compounds, where NOE(E_f) is the number of electrons occupying the states below the Fermi level (E_f).

electronic states lie well below E_f. They form nearly closed spheres. Consequently, the Ti d e_g state seems to be largely unaffected. On their way moving to X, M and R symmetry points, bands 7 and 8 have little energy dispersion until reaching some turning points in the axes. When it happens under the favourable consition that E_f crosses the plane-like section formed by the narrowly missing bands 7 and 8, the denominator in the $X_0(q)$ equation above would become very small. In this case the susceptibility would be mainly determined by the peculiarity in electronic dispersion. The susceptibility of B2 TiAu has two peaks in the [110] direction near $Q_0 = (0.12, 0.12, 0)2\pi/a$ and $Q_0 = (0.45, 0.45, 0)2\pi/a$. It also has a barely visible peak in the [100] direction around $Q_0 = (0.12, 0, 0)2\pi/a$. For B2 TiAu E_f lies at a small distance below the plane-like section formed by bands 7 and 8. This means that the mechanism for TiCu and TiAg discussed above no longer holds for B2 TiAu. TiAu indeed behaves differently from TiCu and TiAg, and its B2 phase exists at high temperatures and it has two forms of low temperature phases (LTPs):B11 and B19 (see, e.g., Massalski *et al* 1986).

The driving mechanisms of the anomalies and the subsequent phase modifications are believed to depend on the subtle features of the Fermi surface (see, e.g., Shabalovskaya 1985, Zhao *et al* 1989). From our $X_0(q)$ results, two types of singularities can be distinguished: type 1, the peak(s) at q around $(1/3, 1/3, 0)2\pi/a$, and type 2, the $q \rightarrow 0$ singularity. For type 1 the distortion may result from the frozen-in transverse acoustic phonons (T_2A) 1/3[110] (Zhao *et al* 1989, Shabalovskaya 1991). The irreducible representations of the space group are characterized by a set of wavevectors corresponding to $q = 1/3\langle 110\rangle$ (Σ points) of the O_h space group. The proper symmetry group for that representation is the point group C_{2v} with 12 equivalent wavevectors (stars): 1/3(011), 1/3(101), 1/3(110), 1/3(011), 1/3(101), 1/3(110) and $q_{i+6} = -q_i (i = 1, \ldots, 6)$. An intermediate phase formed

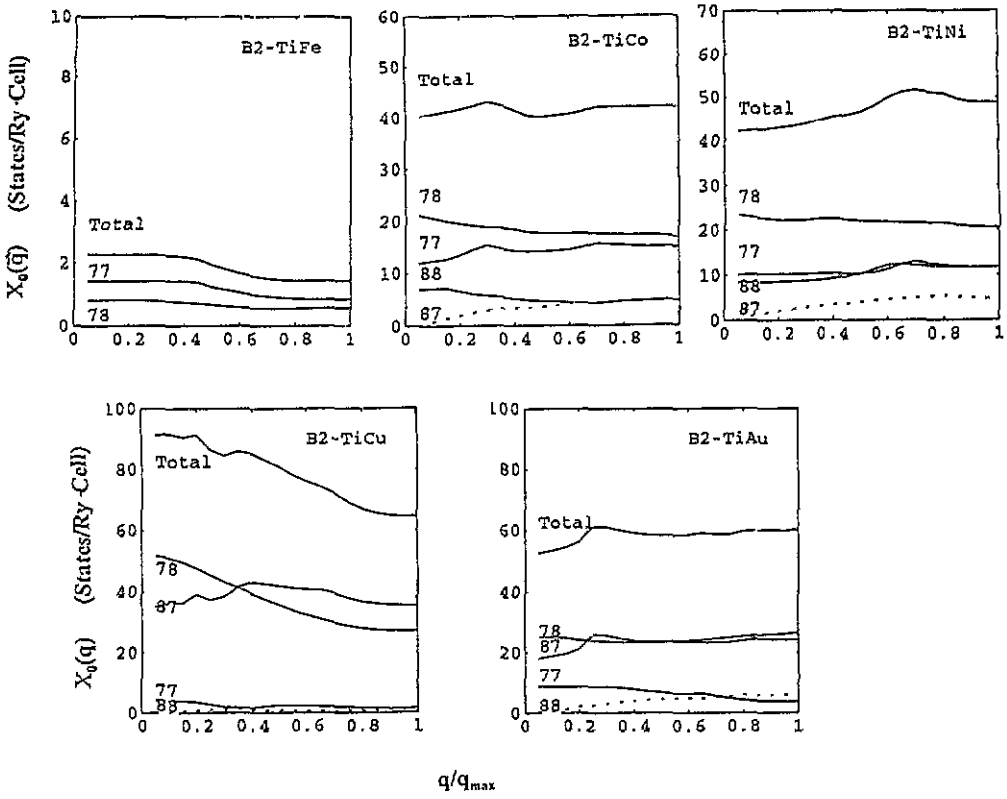

Figure 6. The generalized susceptibility $X_0(q)$ in the [100] direction for the selected B2 TiM compounds.

in this way would fall in the trigonal category (Tietze *et al* 1984, Shapiro *et al* 1984). For type 2 singularity, if the distortion is induced by a single irreducible representation Γ_{12} of O_h and the transformation is a second-order one, one can obtain by minimizing the Landau free energy density with respect to order parameters that there are two and three independent invariants in the symmetry parameters for $l = 4$ and 6, respectively (see, e.g., Haas 1965). The physically possible solutions may be either a tetragonal or an orthorhombic state. The most possible solution is likely to be a simplest distortion: a deviation of c/a from unity. Our study has revealed that instabilties of B2 TiCu and B2 TiAg are caused by the Ti d e_g state. Both of the compounds have stable tetragonal phases. TiRh has been assumed to undergo a distortion from $Pm3m$ to $P4/mmm$ and then a change in the a/b ratio ($P4/mmm$ to $Cmmm$) (Chen and Franzen 1989). However our $X_0(q)$ results fail to show that the transformation could be attributed to the distortion corresponding to a single representation Γ_{12}.

3.4. Low temperature phases (LTPs)

The phase stability eventually should be determined by the total energy difference between the two phases involved. Calculations of the electronic structure for the LTPs are necessary in order to find out whether or not the driving mechanism of the phase transformations discussed above indeed works for the three series. We have performed self-consistent LMTO-ASA total energy calculations for most of the LTPs, including not only the stable

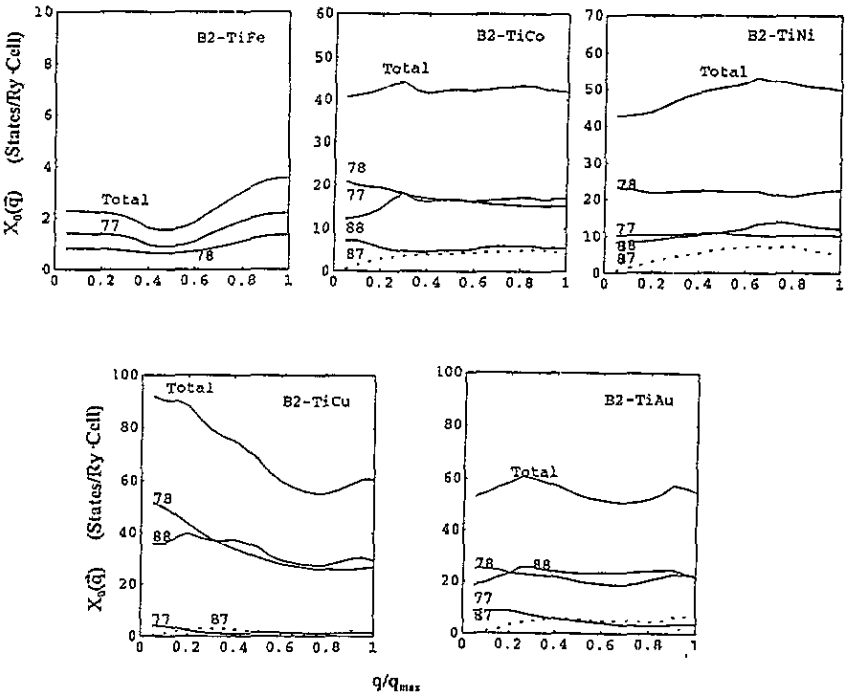

Figure 7. The generalized susceptibility $X_0(q)$ in the [110] direction for the selected B2 TiM compounds.

LTPs listed in table 1 but also the intermediate phases (for example, tetragonal phases for TiRh and TiIr and trigonal phase for TiNi). The LTP studies are more complicated. Their unit cells each contain four atoms and detailed structural information can be found in the references given in table 1. The number of k-points in the IBZ ranges from 400 to 700. The calculated total energy is found to converge well within 0.1 mRyd/unit cell with respect to the number of k-points used and self-consistent cycles. We have found that the combined correction (CC) terms (Skriver 1984) have to be included in order to obtain accurate results. In some cases, for example, for TiPt and TiCu, our calculation without the CC terms failed to give a correct structural modification sequence. Because of the ASA approximation, the LMTO-ASA method may not be well suited for the cases when a shear or an uniaxial strain is applied. Nevertheless, we have found in some cases that the LMTO-ASA method works well when the compound is under deformation. For example, in our tetragonal Bain distortion study for TiRh, TiIr and TiPd compounds, the LMTO-ASA method with CC terms gives results in good agreement with experiments. The main finding from these extensive calculations for the LTPs is that the valence eigenvalue sum (E_{band}) appears to be the major contribution to the lowering of the total energy. This confirms the thermodynamic driving mechanism of the band Jahn–Teller effect nature for the transformations from B2 to LTP as suggested above. Some of the selected results are displayed in figure 8 to illustrate the mechanism of the band Jahn–Teller effect. In comparison with that of B2 TiM, one sees that for LTPs the double-peak-featured DOS for B2 TiM have become more structured and the sharp peaks less pronounced. The DOS(E_f) correspondingly became lower as the bands are split notably around E_f. Detailed report on these LTP calculations is beyond the scope of this paper.

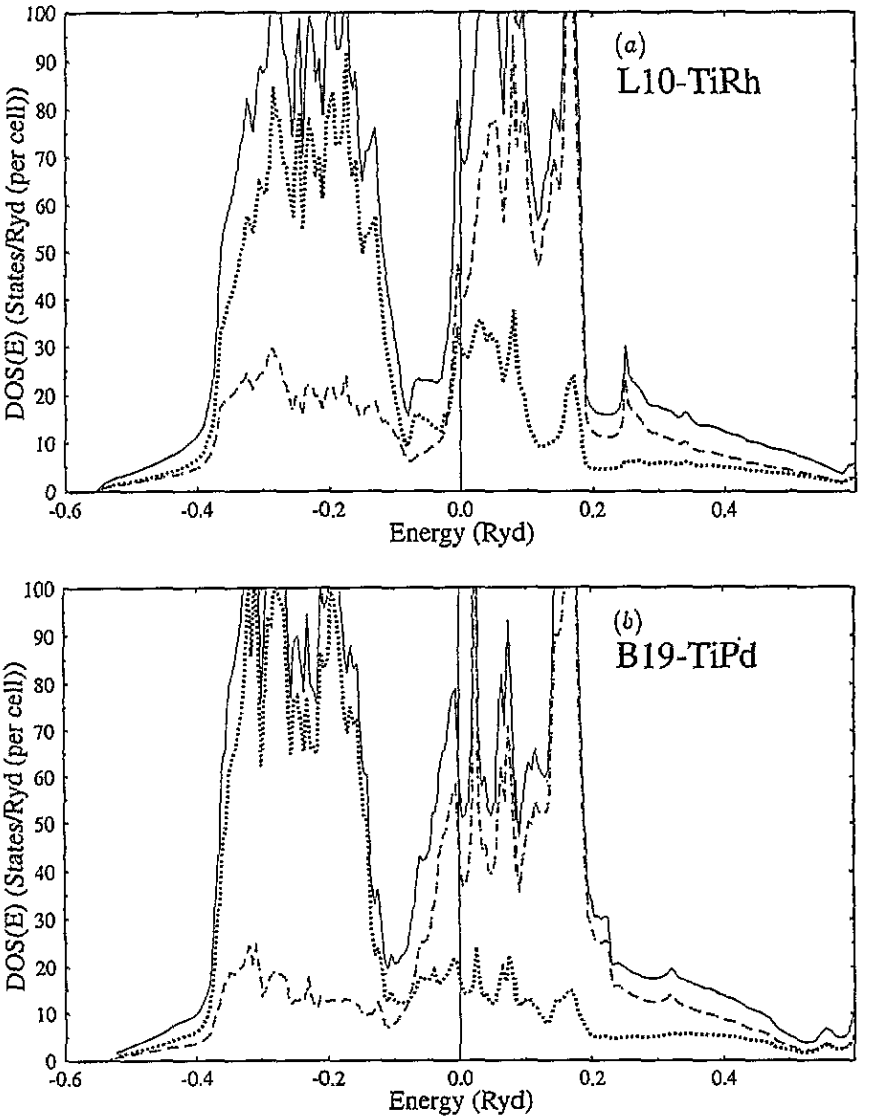

Figure 8. *DOS(E)* of the selected low temperature phases. The Fermi level, E_f, has been designated to be at $E = 0$. Full curve, Total DOS; chain curve, Ti-site DOS; dotted curve, M-site DOS.

4. Conclusion

We have performed first-principles local density functional electronic structure calculations for the 12 B2 TiM compounds using the LMTO-ASA method with the CC terms included. Calculated lattice constants and bulk moduli are in good agreement with measurements. Detailed BS, total and partial DOS, FS and generalized susceptibility have been obtained. A thorough analysis of the possible relationship between the phase instabilities of the B2 structure and the electronic structures has been carried out.

It is found that the instability behaviours of the TiM B2 phases are mainly determined

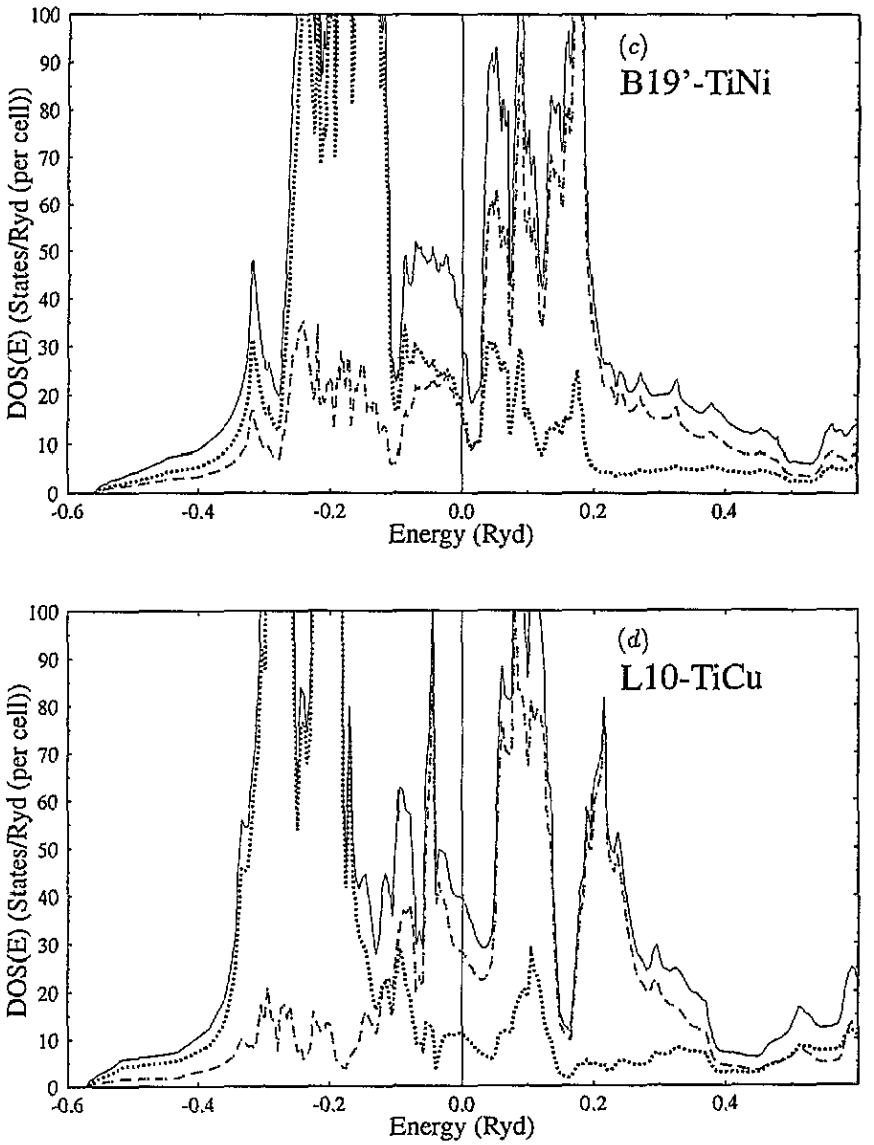

Figure 8. (Continued)

by antibonding M d-band filling. It is also found that the band filling mechanism proposed by Pettifor (1983) to account for the hcp → bcc → hcp → fcc sequence in transition metals also holds for the series of TiM, albeit in a modified form. For the TiM compounds the mechanism appears in the form of the band Jahn–Teller effect. The filling effect of the M d states also plays an important role in shaping the detailed characteristics of the electronic structures. With M becoming more like a filled sphere, its d states becomes more localized, resulting in gradually weakening d–d hybridization with Ti d states. With respect to dynamic mechanisms, our $X_0(q)$ results show two types of singularities: type 1, the peak at the q around $(1/3, 1/3, 0)2\pi/a$, and type 2, the $q \rightarrow 0$ singularity. For type 2, the distortion is induced by a single representation Γ_{12} of O_h and the most possible symmetry change

is from $Pm3m$ to $P4/mmm$. The $X_0(q)$ for B2 TiCu and B2 TiAg show a high peak as $q \rightarrow 0$ and this feature is explained by the peculiarities in their electronic dispersions, but not by the nesting features on the Fermi surfaces. Tetragonal phases with the symmetry $P4/mmm$, which appears to be associated with the $q \rightarrow 0$ singularity, have been observed for TiCu and TiAg. However, this $q \rightarrow 0$ featured driving mechanism may not hold for TiRh.

Finally, we have also performed electronic structure calculations for LTPs. The results corroborate the thermodynamic driving mechanism based on the band Jahn–Teller effect for the transformations from B2 to LTP for the TiM series described above.

Acknowledgments

One of the authors (JMZ) wishes to thank Dr T Sluckin and Professor P T Landsberg for their support, encouragement and valuable suggestions in the past years.

References

Andersen O K 1975 *Phys. Rev.* B **12** 3060
Bihlmayer G, Eibler R and Neckel A 1992 *Ber. Bunsenges. Phys. Chem.* **96** 1626–35
Brandes E A and Brook G B (ed) 1992 *Smithells Metals Reference Book* 7th edn (London: Butterworth-Heinemann)
Brill T M, Mittelbach S, Assmus W, Mullner M and Luthi B 1991 *J. Phys.: Condens. Matter* **3** 9621–7
Chen B H and Franzen H F 1989 *J. Less-Common Met.* **153** L13–9
Colling E W and Gegel H L 1975 *Physics of Solid Solution Strengthening* (New York: Pergamon) p 155
Croeni J G, Armantrout C E and Kato H 1962 Titanium–iridium phase diagram *US Bureau Mines Rep. Invest.* No 6079
Donkersloot H C and Van Vucht J H N 1970 *J. Less-Common Met.* **20** 83–91
Egorushkin V E and Kulkova S E 1982 *J. Phys. F: Met. Phys.* **12** 2823–8
Eibler R, Redinger J and Neckel A 1987 *J. Phys. F: Met. Phys.* **17** 1533–59
Eremenko V N and Shtepa T D 1970 *Russ. Metall. (USSR)* **6** 127–30
Fisher E S and Dever D 1970 *Acta Metall.* **18** 265–9
Folkerts W and Haas C 1989 *J. Less Common. Met.* **147** 181–4
Haas C 1965 *Phys. Rev.* A **140** 863
Hohenberg P and Kohn W 1964 *Phys. Rev.* B **136** 864
Ivanova O P 1990 *Solid State Commun.* **73** 471–5
Karlsson N 1951 *J. Inst. Met.* **79** 391–405
Katahara K W, Manghnani M H and Fisher E S 1979a *J. Phys. F: Met. Phys.* **9** 773–90
Katahara K W, Nimalendran M, Manghnani M H and Fisher E S 1979b *J. Phys. F: Met. Phys.* **9** 2167–76
Kohn W and Sham L J 1965 *Phys. Rev.* A **140** 1133
Kulkova S E, Egorushkin V E and Kalchikhin V V 1991 *Solid State Commun.* **77** 667–70
Lehman G and Taut M 1972 *Phys. Status Solidi* b **54** 469
Lutskaya N V and Alisova S P 1992 *Russ. Metall. (USSR)* **5** 119–21
Massalski T B, Okamoto H, Subramanian P R and Kacprzak L (ed) 1986 *Binary Alloy Phase Diagrams* (Metals Park, OH: ASM International)
Nakanishi N 1979 *Prog. Mater. Sci.* **24** 143
Naumov I I, Velikokhatnyi O I and Bashiron V Z 1991 *JETP Lett.* **54** 573–7
Nevitt M V 1963 *Electronic Structure and Alloy Chemistry of the Transition Elements* ed P A Beck (New York: Interscience)
Papaconstantopoulos D A 1975 *Phys. Rev.* B **11** 4801–7
Papaconstantopoulos D A, Kamm G N and Poulopoulos P N 1982 *Solid State Commun.* **41** 93
Pettifor D G 1983 *Physical Metallurgy* ed R W Cahn and P Hassen (Amsterdam: North-Holland) pp 73–152
Raman A and Schubert K 1964 *Z. Metallkd.* **55** 704–10
Rath J and Freeman A J 1975 *Phys. Rev.* B **11** 2109
Shabalovskaya S A 1985 *Phys. Status Solidi* b **132** 327–44

Shabalovskaya S A 1989 *Solid State Commun.* **70** 23
—— 1991 *Mater. Res. Soc. Symp. Proc.* **246** 247–52
Shabalovskaya S A, Lovkov A I, Narmonev A G and Zakharov A I 1987 *Solid State Commun.* **62** 93
Shabalovskaya S A and Narmonev A G 1988 *Solid State Commun.* **66** 137
Shapiro S M, Fujii Y and Yamada Y 1984 *Phys. Rev.* B **30** 4314
Skriver H L 1984 *The LMTO Method* (Berlin: Springer)
Smithells C J 1962 *Metals Reference Book* 3rd edn, vol 1 (London: Butterworth)
Tietze H, Mullner M and Renker B 1984 *J. Phys. C: Solid State Phys.* **17** L529–32
von Barth U and Hedin L 1972 *J. Phys. C: Solid State Phys.* **5** 1629–42
Yasuda H, Takasugi T and Koiwa M 1991 *Mater. Trans. JIM* **32** 48–51
Yi S S, Chen B H and Franzen H F 1988 *J. Less-Common Met.* **143** 243–9
Zhao G L, Leung T C and Harmon B N 1989 *Phys. Rev.* B **40** 7999–8001